Computing with Discrete Models of Ruled Surfaces and Line Congruences

Boris Odehnal and Helmut Pottmann
Institute of Geometry, Vienna University of Technology
Wiedner Hauptstr. 8-10, A-1040 Wien, Austria

April 18, 2001

Abstract

Geometric computing based on discrete models turned out to be highly effective for many applications in Computer Graphics and Geometric Modeling. The present paper discusses algorithms for discrete models of ruled surfaces and line congruences, and outlines applications in robotics and CNC machining. The problems addressed are estimation of invariants from discrete models and interpolatory variational subdivision algorithms.

1 Introduction

In geometric computing, discrete models of curves and surfaces play an increasingly important role. In part this is due to the easy availability of storage capacity: it is no longer necessary to store a surface via the control nets of patches. It is possible to store and process a rather dense polyhedral approximation. In particular in connection with subdivision algorithms and multiresolution representations, this is an attractive alternative to the freeform surface approach, especially for applications in computer graphics and scientific visualization. This is our motivation for discussing *discrete models of ruled surfaces and congruences of lines.*

Ruled surfaces appear for example in motion planning, e.g., for welding robots, CNC machining [9] or wire cut EDM [13]. For 5-axis CNC-machining it recently turned out that congruences which contain the axis positions of the moving tool are of importance [15]. For these applications it is actually not necessary to have a complete description of the ruled surface, line congruence or robot motion. It is sufficient to be able to compute a sufficiently dense discrete model.

A discrete ruled surface model consists of a sequence of lines $R_0, R_1, \ldots$, which algorithms of geometric processing are applied to. Invariants of Euclidean differential geometry of ruled surfaces can be approximated by appropriate invariants of the discrete model. This is the subject of so-called *difference geometry* [14].

The present paper is a contribution to *computational line geometry.* This research direction has been initiated particularly by B. Ravani et al. [4, 13] and further developed recently [10, 11]. Computational line geometry, its classical geometric background and applications in various areas, particularly CAGD and robotics, are the subject of a monograph by H. Pottmann and J. Wallner [12].

2 Discrete Counterparts of Differential Geometric Invariants of Ruled Surfaces

In order to describe some basics of difference geometry of ruled surfaces we introduce the following notations (see Fig. 1). Consecutive lines R_i, R_{i+1} enclose the angle $\phi_{i,i+1}$ and possess the common perpendicular $N_{i,i+1}$. The distance $h_{i,i+1}$ of the lines R_i, R_{i+1} equals the distance of the two footpoints $f_{i,i+1} \in R_i$ and $f_{i+1,i} \in R_{i+1}$. The line R_i is incident with the footpoints $f_{i,i-1}$ and $f_{i,i+1}$. We will now illustrate the computations with discrete ruled surface models by

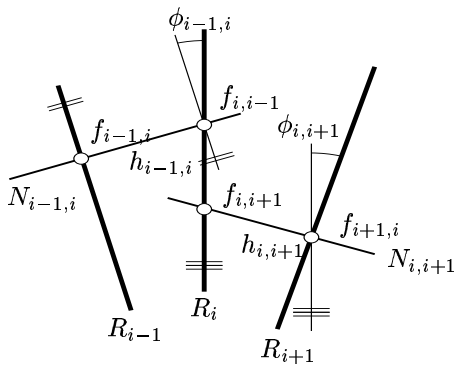

Figure 1: Discrete ruled surface model: Notations.

means of the *striction curve.* For a smooth ruled surface with rulings $R(u)$, we denote the *striction point* by $s(u)$. The striction point $s(u)$ is that point of a ruling $R(u)$, where the Gaussian curvature reaches its maximum [5, 6]. For a developable ruled surface, or a torsal ruling (i.e., ruling with a constant tangent plane) of a skew ruled surface, the striction point is a singular surface point. Therefore, the striction curve, which is formed by the striction points, is an important geometric property of the ruled surface. There are other, equivalent definitions of the striction point, one of which will follow from the discussion below. Furthermore, let $\delta(u)$ be the *distribution parameter.* The distribution parameter measures the winding of the tangent planes along a ruling. It is

zero for a torsal ruling, in particular for all rulings of a developable surface. Otherwise, it equals half of the distance of those two points on the ruling, whose midpoint is the striction point and whose tangent planes form a right angle.

Finally, let $s(u)+\lambda e_3(u)$ be the *central tangent*. This is the surface tangent at the striction point, which is orthogonal to the ruling. The distribution parameter is zero for a torsal ruling, in particular for all rulings of a developable surface. It will turn out that the points $f_{i,i+1}$ and f_{i,i_1} are discrete analogues of the striction points. We further define the discrete distribution parameter

$$\delta_{i,i+1} := \frac{h_{i,i+1}}{\phi_{i,i+1}}. \tag{1}$$

We assume that there is a smooth ruled surface with generators $R(u)$ such that $R_i = R(u_i)$ with $u_0 < u_1 < u_2 < \ldots$, and study the behaviour of $f_{i,i+1}$, $f_{i+1,i}$, and $h_{i,i+1}$ as u_{i+1} converges to u_i. The following proposition summarizes well-known facts concerning the discrecte ruled surface model, see [14].

Proposition 1: *Assume that $R(t)$ is the family of rulings of a twice continously differentiable ruled surface R, and let $R_i = R(u)$, $R_{i+1} = R(u+h)$. Then*

$$\delta(u) = \lim_{h\to 0} \delta_{i,i+1}, \tag{2}$$

$$s(u) = \lim_{h\to 0} f_{i,i+1} = \lim_{h\to 0} f_{i,i-1}, \tag{3}$$

$$s(u) + [e_3(u)] = \lim_{h\to 0} N_{i,i+1}. \tag{4}$$

Proof: We assume that R is parametrized by $x(u,v) = s(u) + ve(u)$, where $s(u)$ is the striction line, and that $\|\dot{s}(u)\| = \|e(u)\| = 1$. Without loss of generality we let $u = 0$ and let $s(h) = s(0) + h\dot{s}(0) + (h^2/2)\ddot{s}(0) + o(h^2)$, and $e(h) = e(0) + h\dot{e}(0) + o(h)$.

It is a matter of elementary linear algebra to compute $\delta_{i,i+1}$ and $f_{i,i+1}$. We have

$$h_{i,i+1} = \det(s(h) - s(0)), e(h), e(0))/\|e(h) \times e(0)\|),$$
$$\text{and} \qquad \phi_{i,i+1} = \angle(e(h), e(0)) = h\|\dot{e}(0)\| + o(h),$$

which shows that

$$\delta_{i,i+1} = \det(\dot{s}(0), e(0), \dot{e}(0)) + o(1). \tag{5}$$

Analogously, we compute $f_{i,i+1}$. If $f_{i,i+1} = s(0) + f(h)e(0)$, then

$$f(h) = -he(0)\dot{s}(0) + o(h). \tag{6}$$

Equ. (5) shows (2) by comparison with a well-known formula from line geometry [6, 12]. Analogously, equ. (6) shows that $\lim_{h\to 0} f(h) = 0$, which implies (3). Equ. (4) is a consequence of (3), because the line $N_{i,i+1}$ must now converge to a surface tangent orthogonal to the ruling $R(u)$. □

The footpoints of the common perpendiculars of neighboring rulings converge to the striction points. On each ruling we have two such footpoints, $f_{i,i+1}$ and $f_{i,i-1}$. Either one can be used in a discrete model of the striction curve. However, it turns out that the midpoint of the two footpoints is a much better approximation:

Proposition 2: *For a discrete ruled surface model, we have*

$$s(u) = \lim_{h\to 0} \frac{1}{2}(f_{i,i+1} + f_{i,i-1}), \quad \delta(u) = \lim_{h\to 0} \frac{1}{2}(\delta_{i-1,i} + \delta_{i,i+1}), \tag{7}$$

and the convergence is quadratic.

Proof: We use the notations of the proof of the previous proposition. Equations (5) and (6) show that both $\delta_{i,i+1}$ and $f_{i,i+1}$ are smoothly dependent on h. We write $\delta(h)$ for $\delta_{i,i+1}$. Then $\delta_{i,i+1} = \delta(h) = \delta(0) + h\dot{\delta}(0) + o(h)$, and $\delta_{i-1,i} = \delta(-h) + \delta(0) - h\dot{\delta}(0) + o(h)$. This shows that

$$\frac{1}{2}(\delta_{i-1,i} + \delta_{i,i+1}) = \delta(0) + o(h),$$

which means that the convergence of the left hand side of this equation towards $\delta(0)$ is quadratic in h. The same argument applies for $f(h)$ and we are done. □

Because of the quadratic convergence of the midpoint of the two footpoins $f_{i,i+1}$ and $f_{i-1,i}$ to the striction curve, we use the sequence of these midpoints as a discrete model for the striction curve. **Example 1:** Figure 2 shows a discretized

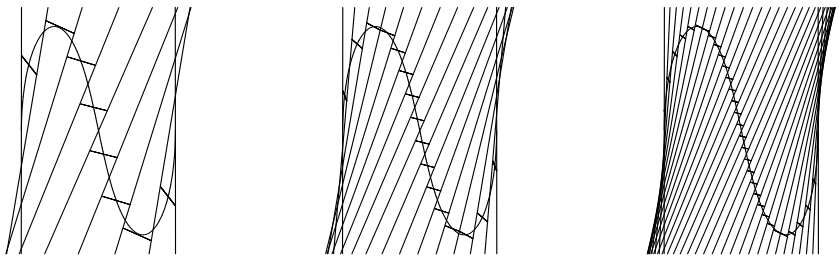

Figure 2: Discrete model of a ruled surface with striction line and sequence of common normals of generators

ruled surface with striction line. We choose one of the two reguli contained in the hyperboloid

$$\frac{x^2}{1} + \frac{y^2}{4} - \frac{z^2}{9} = 1,$$

discretize it and show the polygon built by the midpoints of the footpoints $f_{i,i+1}$ and $f_{i+1,i}$ in Figure 3. Also the other invariants of ruled surfaces can be expressed at hand of the discrete model. The interested reader may find this in the monograph on difference geometry by R. Sauer [14]. Investigations of

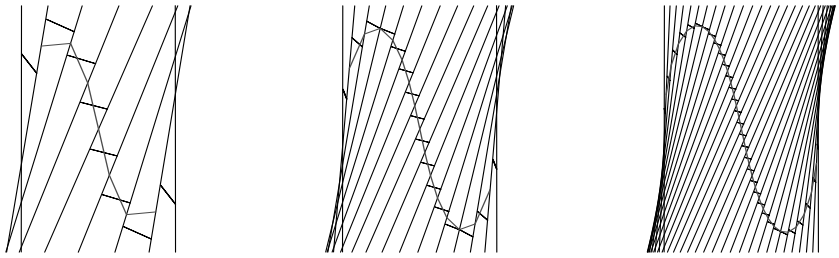

Figure 3: Discrete model of ruled surface with discrete central curve

descrete approximants of differential invariants, espacially with regard to the convergence order, would be a rewarding future research topic. We mention here one paper in this direction [16], which studies the convergence order of discrete curvature estimates.

3 Isometric Mappings and Approximate Development of Ruled Surfaces

The difference geometric approach also nicely visualizes *isometric mappings* between ruled surfaces [14]. Here we focus on so-called *Minding isometries* [6], which map rulings to rulings.

Consider a discrete ruled surface $R_0, R_1, \ldots$ and a polygon $p_0, p_1, \ldots$ with vertices $p_i \in R_i$, which should be a *discrete curve* contained in the ruled surface.

If this discrete model comes from discretizing an actual smooth ruled surface $R(t)$ and a rectifiable curve $c(t) \in R(t)$, i.e., we have $t_0 < t_1 < \ldots$ and $R_i = R(t_i)$ and $p_i = c(t_i)$, then the length of the polygon $p_0, p_1, p_2, \ldots$, converges to the arc length of the curve $c(t)$, if $t_i - t_j$ tends to zero uniformly. Mappings of one discrete model onto another, which preserve the edge lengths of all polygons are therefore discrete versions of isometric mappings of ruled surfaces. Such transformations are constructed as follows: We consider a pair R_i, R_{i+1} of consecutive rulings as a rigid body $S_{i,i+1}$, and the common perpendicular $N_{i,i+1}$ is assumed to be part of this rigid body. We think of the ruling R_i as a hinge which connects $S_{i-1,i}$ and $S_{i,i+1}$. In this way these two adjacent bodies can rotate freely about the line R_i.

We obtain a kinematic chain whose internal degree of freedom equals the number of hinges, i.e., the number of rulings R_i minus the first and the last one. All transformations of discrete models which are composed of such a sequence of rotations about the lines R_i preserve the arc length of all discrete polygons $p_0, p_1, \ldots$ with $p_i \in R_i$. We therefore use these mappings as discrete models

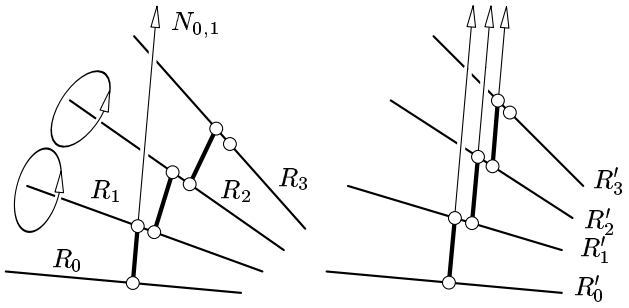

Figure 4: Discrete ruled surface model (left) and conoidal model isometric to the first one (right)

of the Minding isometries of ruled surfaces. **Example 2:** As an example, let

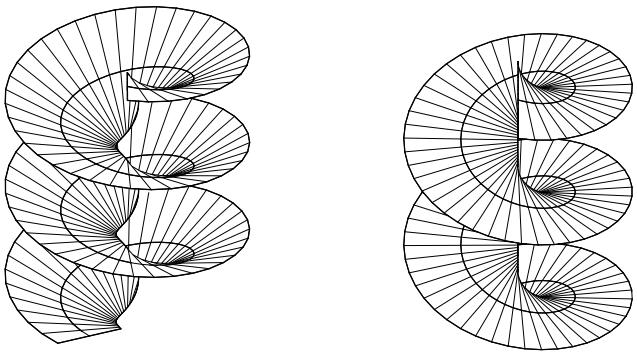

Figure 5: Left: Ruled helical surface. Right: Isometric conoidal surface. In this case the result is a helical surface whose generators intersect the axis orthogonally.

us use the discrete model to show that *any ruled surface can be isometrically mapped onto a conoidal ruled surface.* Recall that by definition all rulings of a conoidal ruled surface are parallel to a certain fixed plane.

We assume a discrete model $R_0, R_1, \ldots$ and fix the first two rulings R_0, R_1. Then the rigid body $S_{1,2}$ composed of R_1,R_2 is rotated about R_1 until the common perpendicular $N_{1,2}$ becomes parallel to $N_{0,1}$. We continue in this way, until all common perpendiculars $N_{i,i+1}$ are parallel to $N_{0,1}$.

The new discrete model $R'_0 = R_0, R'_1 = R_1, R'_2, \ldots$ has the property that all its rulings R'_i are orthogonal to $N_{0,1}$, and therefore parallel to the plane spanned by R_0 and R_1. This means that $R'_0, R'_1, \ldots$ is a discrete model of a conoidal ruled surface, see Figure 4.

It is not difficult to show that if the original rulings R_i come from an actual smooth ruled surface R, and we use finer and finer discrete models, this proce-

dure actually converges to a conoidal surface which is isometric to R, see Figure 5.

If we apply the procedure described by Example 2 to a developable surface, we get its development. Thus we may compute an *approximate development* of a

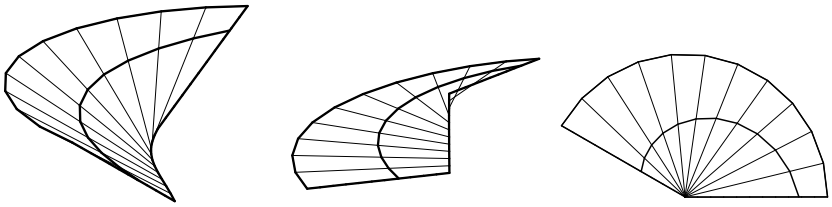

Figure 6: Approximate development of a skew ruled surface based on the discrete representation: Left: Discrete model of a skew ruled surface. In the middle: Isometric conoidal discrete model. Right: Projection of the discrete conoidal surface orthogonal to its generators.

skew ruled surface, which is desirable in certain applications [1], as follows, see Figure 6: *First compute the isometric conoidal surface (e.g., by using a discrete model), and then project orthogonally onto a plane parallel to the rulings.* This mapping is isometric if restricted to any of the rulings. Moreover, we see that the striction curve of the original surface is mapped to the striction curve of the conoidal surface. It is well known that the orthogonal projection of a conoidal surface onto a reference plane (a plane which is parallel to the rulings) maps the striction curve to the envelope of the projected rulings. For developable surfaces, the regression curve (striction curve) is mapped to the envelope of the rulings in the exact development. It is interesting that we have a similar property for the proposed approximate development. Note also that the isometry to a conoidal surface can be used to check how much a certain ruled surface R differs from a developable surface: The isometric conoidal surface R' should not differ much from a plane. The extremal distance between two rulings of R', the 'height' of this surface, is a measure of non-developability.

Using difference geometry, many variants and improvements of such an approximate development are possible. For a discussion of the approximate development of ruled surface strips near their striction curve, see G. Aumann [1].

4 Subdivision Algorithms for Ruled Surfaces

A subdivision algorithm computes a refined discrete model from a coarser one. We are going to study subdivision algorithms which converge to smooth ruled surfaces. One type of subdivision algorithms recomputes a refinement from coarse data ones, but does nott keep all input data. An example of this is *Chaikin's algorithm*, see Figure 7. It produces a sequence of polygons which

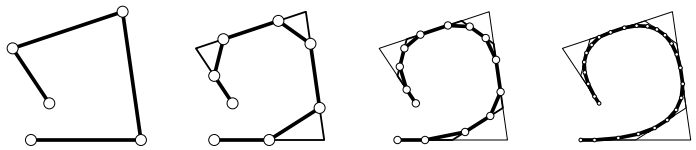

Figure 7: Chaikin's algorithm.

converges to a quadratic B-spline curve with uniform knot vector and the original input points $p_0, \ldots, p_n$ as control points, see Figure 7. Note that the limit curve touches the interior edges of the control polygon in their midpoints. The algorithms of de Casteljau and de Boor are subdivision algorithms of this type as well. Their repeated application yields a sequence of polygons which converges towards a Bezier curve or B-spline curve, respectively [7].

Subdivision algorithms for ruled surfaces and line congruences, which imitate the behaviour of the algorithms of de Casteljau and de Boor have been investigated by Ravani et al. [4, 13].

Another type of subdivision algorithm computes a refinement, which contains the original input data. Clearly, this leads to geometric models which interpolate the given data and is thus called an *interpolatory subdivision scheme*. One of the first schemes of this kind has been found by Dyn, Levin and Gregory [3]: Let w be a real number, which acts as a shape parameter. From four consecutive points $p_{i-1}, \ldots, p_{i+2}$ of a polygon Dyn et al. compute the point $p_{i+1/2}$ according to

$$p_{i+1/2} = (\frac{1}{2} + w)(p_i + p_{i+1}) - w(p_{i-1} + p_{i+2}). \tag{8}$$

The refined polygon then has vertices $\ldots p_i, p_{i+1/2}, p_{i+1}, \ldots$. Dyn et al. have proved that this subdivision scheme produces polygons which converge to a C^1 curve for $0 < w < \frac{1}{8}$. An example is shown in Figure 8. Polygonal subdivi-

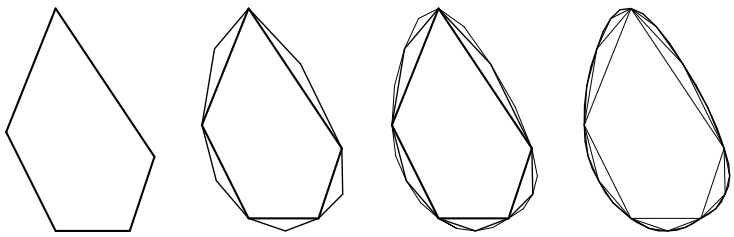

Figure 8: Interpolatory subdivision according to Dyn, Levin and Gregory ($w = 1/13$).

sion schemes can be used to generate discrete models of ruled surfaces: Given a sequence of line segments $p_i q_i$, $(i = 0, \ldots, n)$, we apply the same subdivision scheme to both boundary polygons $p_0, \ldots, p_n$ and $q_0, \ldots, q_n$. Connecting

corresponding points of the refined polygon gives a refined sequence of line segments. Smoothness of the limit surface is guaranteed if the two limit polygons are smooth.

If no line segments but entire lines are given, we can apply polygonal subdivision algorithms by selecting appropriate segments, e.g., segments of constant length which lie symmetric to the footpoints $f_{i,i-1}$ and $f_{i,i+1}$. More sophisticated methods, which involve variational principles, can be found in [12].

Reducing the computation of a surface to the computation of two curves contained in it without looking at the surface itself may not be the best solution. Hence, we propose the following *variational interpolatory subdivision for ruled surface strips.*

Let R_i with $1 \leq i \leq N$ be a set of generators of a ruled surface R. We think of R as a strip bounded by two curves a and b, and span R_i by the points a_i and b_i. We want to insert a new generator $R_{i,i+1}$ between each pair (R_i, R_{i+1}) of consecutive generators. The end points of $R_{i,i+1}$ shall be denoted by A_i and B_i, respectively. For the notations, see Figure 9. Now the old and new line

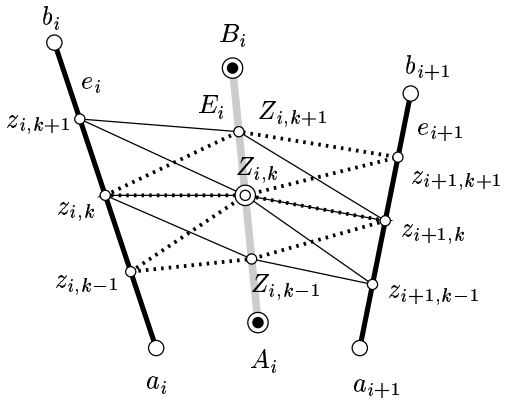

Figure 9: Basic notations for a subdivided ruled surface strip, the two different triangulations.

segments are divided into n equal parts. We get the points

$$z_{i,k} := \frac{n-k}{n} a_i + \frac{n}{k} b_i, \tag{9}$$

$$Z_{i,k} := \frac{n-k}{n} A_i + \frac{n}{k} B_i. \tag{10}$$

These points together define two different triangulations on R, see Figure 9. In this triangulation each point $Z_{i,k}$ which is no boundary point, i.e. $k \neq 0, n$, has exactly six neighbouring points

$$Z_{i,k-1}, Z_{i,k+1}, z_{i,k}, z_{i,k-1}, z_{i+1,k+1}, z_{i+1,k}, \tag{11}$$

$$Z_{i,k-1}, Z_{i,k+1}, z_{i,k}, z_{i,k+1}, z_{i+1,k-1}, z_{i+1,k} \tag{12}$$

with respect to the two triangulations. In this triangulated ruled surface model,

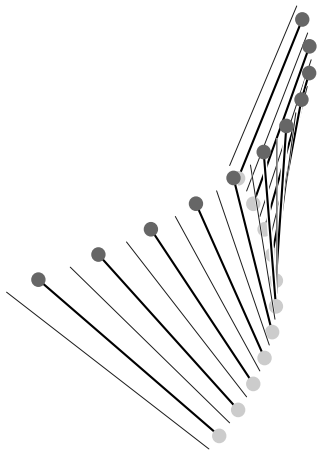

Figure 10: 12 generators taken out of a quartic ruled surface R, 11 lines inserted; light gray spheres centered at A_i, dark gray spheres centered at B_i.

the so-called *umbrella vectors* of $Z_{i,k}$ can be computed as

$$U_{i,k} := Z_{i,k} - \frac{1}{6}\left(Z_{i,k-1} + Z_{i,k+1} + z_{i,k} + z_{i,k-1} + z_{i+1,k+1} + z_{i+1,k}\right) \qquad (13)$$

$$\widetilde{U}_{i,k} := Z_{i,k} - \frac{1}{6}\left(Z_{i,k-1} + Z_{i,k+1} + z_{i,k} + z_{i,1+1} + z_{i+1,k-1} + z_{i+1,k}\right), \qquad (14)$$

again with respect to the two triangulations. The umbrella vector has been introduced by L. Kobbelt [8]. Its Euclidean norm can be seen as a discrete measure for the absolute value of the mean curvature in the neighbourhood of $Z_{i,k}$. Now the points A_i and B_i which span the lines $R_{i,i+1}$ will be chosen such that the following "discrete energy functional" is minimized,

$$F = \sum_{i,k} (U_{i,k}^2 + \widetilde{U}_{i,k}^2). \qquad (15)$$

F is quadratic in the unknown coordinates of A_i, B_i, and thus the minimization problem amounts to the solution of a linear system.

Example 3: As an example we take $N = 12$ generators from a quartic ruled surface $R(u,v) = (1 + vu^2, u^2/2 + uv, u - v)$ and let $n = 12$. The result of one step of the variational subdivision is shown in Figure 10.

We did not prove the convergence of this interpolatory subdivision scheme. However, it seems to be irrelevant for practical applications, since after a few iterations of the variational scheme any known convergent subdivision scheme, applied independently to the boundary polygons, will produce satisfactory results.

5 Subdivision Schemes for Congruences of Lines

Line congruences are smooth 2-parameter manifolds of lines. As an example, consider the positions of the axis of a cutting tool. They might have been computed in order to yield good local cutting conditions, e.g. in order to result in small scallop heights. We use a double indexed-sequence R_{ij} of lines as a discrete model for a line congruence. Now we want to refine this set of axis positions. Higher density of lines is required for the definition of smooth motions of the cutter and it yields better control during the milling process.

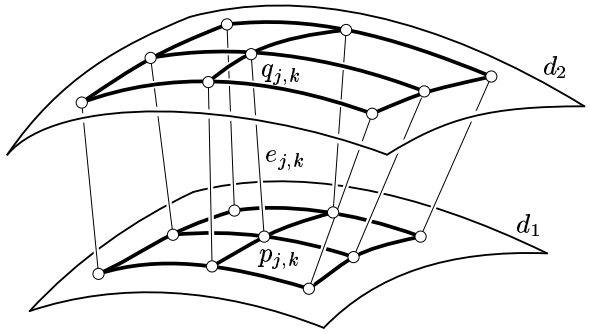

Figure 11: Congruence of lines determined by two directrices

The area of interest in which we consider the line congruence shall be bounded by two director surfaces d_1 and d_2, respectively. Furthermore, we assume that the intersection points of the lines with d_i, and therefore the lines themselves, can be arranged in the way shown in Figure 11.

5.1 Interpolatory Subdivision

The intersection points $p_{i,j}$ of $R_{i,j}$ with the directrix d_1 can be triangulated as shown in Figure 12. Now we use the *butterfly scheme* to insert new points $\overline{p}_{i,j}$ on the edges which connect $p_{i,j}$ with $p_{i+1,j+1}$, where

$$\begin{aligned}\overline{p}_{i,j} := \tfrac{1}{2}(p_{i,j} + p_{i+1,j+1}) + 2w(p_{i+1,j} + p_{i,j+1}) - \\ -w(p_{i,j-1} + p_{i-1,j} + p_{i+1,j+2} + p_{i+2,j+1})\end{aligned} \tag{16}$$

and w serves as tension parameter. The same can be done with the intersection points $q_{i,j}$ of $R_{i,j}$ with d_2. So the subdivision algorithm for line congruences is a composition of the subdivision algorithms done for the endpoints of the line segments. **Example 4:** To demonstrate how this subdivision scheme works on congruences of lines we choose two different director surfaces d_1. The surface d_2 which is a generalized offset surface in both cases is not plotted in Figure 13 since it is only necessary to determine the direction of the lines in the congruence. The congruences in the examples differ from normal congruences, as is seen in

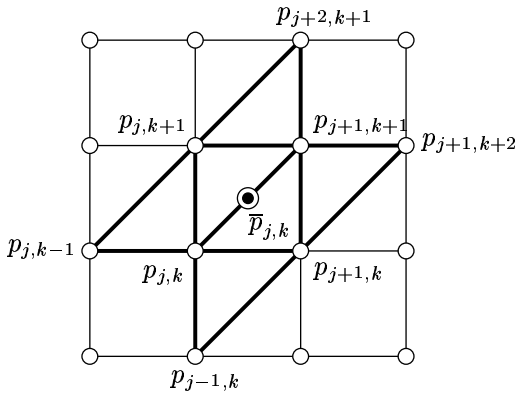

Figure 12: The butterfly-scheme

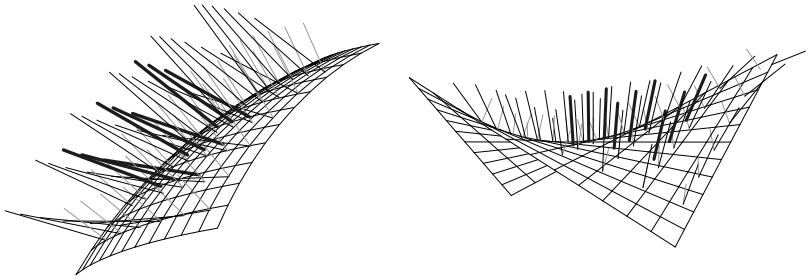

Figure 13: Left: part of a sphere with lines of the congruence (black, thin), inserted lines (black, thick). Right: part of a hyperbolic paraboloid, lines of the congruence (black, thin), inserted lines (black, thick).

Figure 13. Since we did not insert points on the edges connecting $p_{i,j}$ with $p_{i+1,j}$ and $p_{i,j}$ with $p_{i,j+1}$, respectively, we did not insert lines into the boundaries of the domain $D_{i,j} := \{p_{i,j}, p_{i+1,j}, p_{i+1,j+1}, p_{i,j+1}; q_{i,j}, q_{i+1,j}, q_{i+1,j+1}, q_{i,j+1}\}$. If the union of all these domaines forms a smooth congruence of lines, they were joined along smooth ruled surfaces and it is possible to apply the technique described in section 4 to insert lines to the regions which were not reached by the butterfly scheme.

5.2 Variational Subdivision

Another possibility to insert lines into a given discrete congruence is to combine least square methods and interpolatory subdivision.

Again we assume the lines $R_{i,j}$ with $1 \leq i \leq N_1$ and $1 \leq j \leq N_2$ to be determined by their intersection points $p_{i,j}$ and $q_{i,j}$ with the director surfaces d_1 and d_2, respectively. Furthermore, we assume that the points $p_{i,j} \in d_1$ and

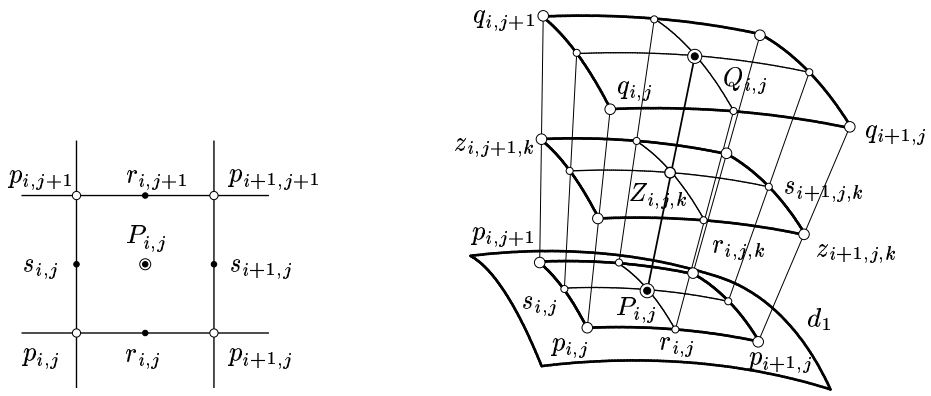

Figure 14: Point scheme on directrix surface d_1 (left), part of the congruence with some notations (right).

$q_{i,j} \in d_2$ can be arranged in a quadrangular scheme as shown in Figure 14. Therefore the discrete congruence of lines can be seen as two one-parameter families of discrete ruled surfaces.

We can appply the variational subdivision technique which was described in section 4 onto these *discrete congruence surfaces* in order to insert new lines $T_{i,j}$ with $1 \leq i \leq N_1 - 1$ and $1 \leq j \leq N_2 - 1$ and $S_{i,j}$ with $1 \leq i \leq N_1$ and $1 \leq j \leq N_2 - 1$ respectively. We denote the intersection points of $T_{i,j}$ and $S_{i,j}$ with the director surfaces by $r_{i,j}$, $r'_{i,j}$ and $s_{i,j}$, $s'_{i,j}$, respectively.

Now we want to insert lines $\overline{R}_{i,j}$ with $1 \leq i \leq N_1 - 1$ and $1 \leq j \leq N_2 - 1$ into the interior of the hexahedral regions formed by the line segments $R_{i,j}$, $R_{i+1,j}$, $R_{i+1,j+1}$ and $R_{i,j+1}$. The new lines $\overline{R}_{i,j}$ will have intersection points $P_{i,j} \in d_1$ and $Q_{i,j} \in d_2$ with the respective directrix surfaces.

We divide the given lines and the lines $T_{i,j}$ and $S_{i,j}$ into K equal parts, which gives the points

$$\begin{aligned} z_{i,j,k} &:= (1 - \frac{k}{K})p_{i,j} + \frac{k}{K}q_{i,j}, \\ a_{i,j,k} := (1 - \frac{k}{K})r_{i,j} + \frac{k}{K}r'_{i,j}, &\quad b_{i,j,k} := (1 - \frac{k}{K})s_{i,j} + \frac{k}{K}s'_{i,j}. \end{aligned} \tag{17}$$

We also divide the lines $\overline{L}_{i,j}$ into K equal parts and get the points

$$Z_{i,j,k} := (1 - \frac{k}{K})P_{i,j} + \frac{k}{K}Q_{i,j}. \tag{18}$$

Now each point $Z_{i,j,k}$ in the K discrete director surfaces defined by $k = const.$ has eight neighbours. These are the points

$$z_{i,j,k},\ z_{i+1,j,k},\ z_{i+1,j+1,k},\ z_{i,j+1,k},\ r_{i,j,k},\ r_{i,j+1,k},\ s_{i,j,k},\ s_{i+1,j,k}, \tag{19}$$

which define the umbrella vector of $Z_{i,j,k}$ as

$$U_{i,j,k} := Z_{i,j,k} - \frac{1}{8}(z_{i,j,k} + z_{i+1,j,k} + z_{i+1,j+1,k} + \\ + z_{i,j+1,k} + r_{i,j,k} + r_{i,j+1,k} + s_{i,j,k} + s_{i+1,j,k}), \tag{20}$$

where $1 \leq i \leq N_1 - 1$, $1 \leq j \leq N_2 - 1$ and $0 \leq k \leq K$.

The umbrella vectors $U_{i,j,k}$ make it possible to define a "discrete energy functional" for the discrete congruence of lines by

$$F := \sum_{i,j,k} U_{i,j,k}^2. \tag{21}$$

F is a quadratic function in the unknown coordinates of the $(N_1 - 1)(N_2 - 1)$ points $P_{i,j}$ and $Q_{i,j}$ and thus this minimization problem amounts to the solution of a linear system. **Example 5:** We take $d_1 = (u, v, \frac{1}{2}\sin(2u + 1.5v))$

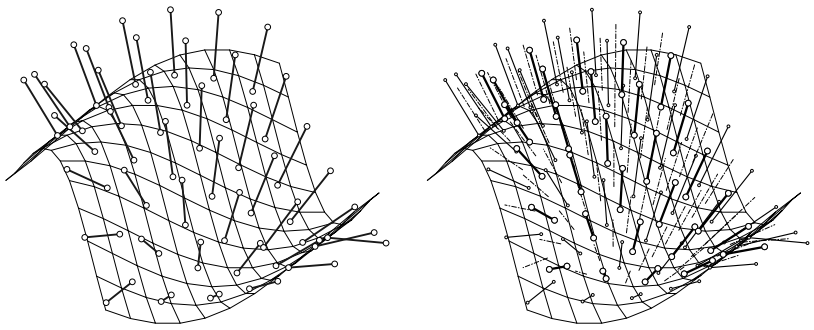

Figure 15: Discrete congruence of lines (left), inserted lines (black thick) (right).

as directorurface of a cogruence of lines and choose the lines $L(u, v)$ incident with $d_1(u, v)$ and parallel to $(u, v, \sin u + 1.3 \cos v)$. The lines $L_{i,j}$ correspond to 8×7 values (u, v) of a regular rectangular grid in the square $[-1.1, 1.1]^2$. We let $K = 6$. The result of variational subdivision for line congruences can be seen in Figure 15.

The convergence of this variational subdivision needs to be proofed

Example 6: As an example of practical importance we look at a profile which we want to mill. Some axis positions of the milling tool are given, see Figure 16 (the dark line segments). We demonstrate that a few steps of our variational subdivision can produce a smooth path for a milling tool.

Therefore we proceed as described in section 4. Figure 16 also shows the inserted lines (the light ones). Figure 16 shows the profile and the milling toll in action after the first step of the variational subdivision. The curve built by the barycenter of the cutting tool is also shown. Figure 17 shows a further refinement of the discrete ruled surface composed of the axis and the resulting profile.

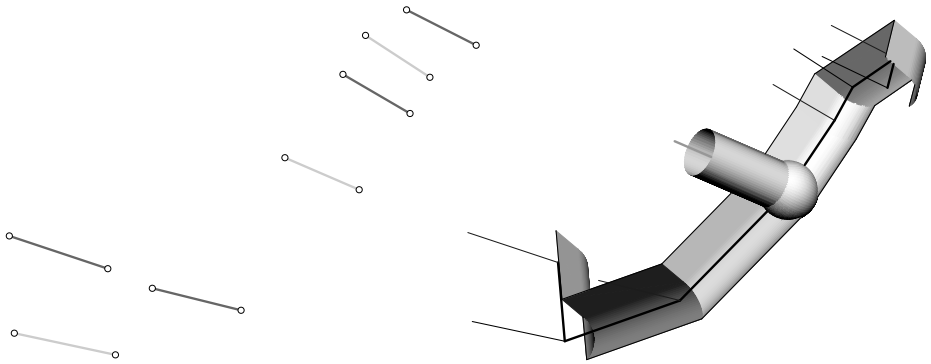

Figure 16: First step of the refinement

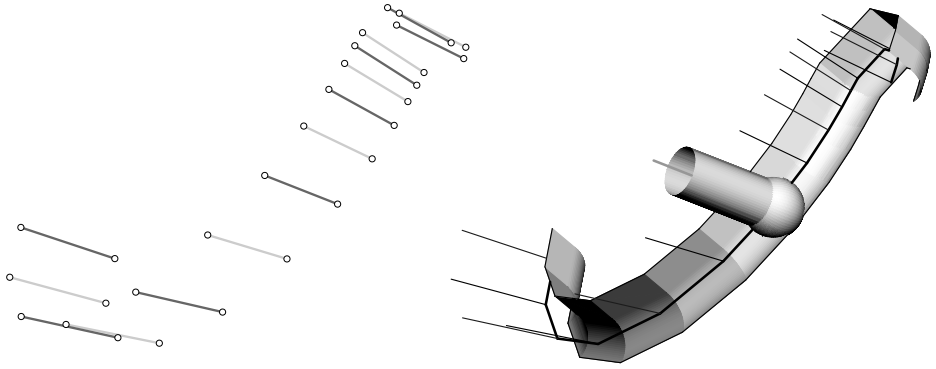

Figure 17: Second step of the refinement

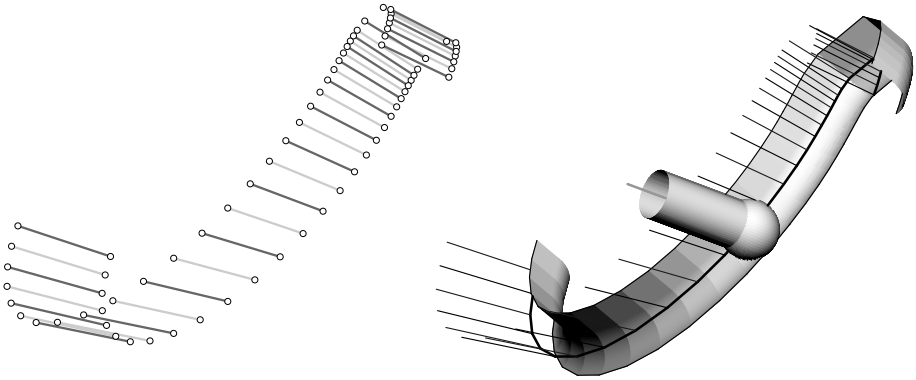

Figure 18: Third step of the refinement

Acknowledgement: This research has been supported by grant P-13648-MAT of the Austrian Science Fund.

References

[1] Aumann, G., Approximate development of skew ruled surfaces, Computers & Graphics **13** (1989), 361–366.

[2] Dyn, N., Gregory, J. and Levin, D., A 4-point interpolatory subdivision scheme for curve design, Comp. Aided Geom. Design **4** (1987), 257–268.

[3] Dyn, N., A butterfly subdivision scheme for surface interpolation with tension control, ACM Trans. on Graphics **9** (1990), 160–169.

[4] Ge, Q.J. and Ravani, B., Geometric design of rational Bézier line congruences and ruled surfaces using line geometry, Computing **13** (1998), 101–120.

[5] Hlavaty, V., Differential Line Geometry. P. Nordhoff Ltd., Groningen 1953.

[6] Hoschek, J., Liniengeometrie. Bibliograph. Institut, Zürich 1971.

[7] Hoschek, J. and Lasser, D., Fundamentals of Computer Aided Geometric Design, A. K. Peters, Wellesley, MA 1993.

[8] Kobbelt, L., Iterative Erzeugung glatter Interpolanten, Dissertation, Karlsruhe, 1994.

[9] Marciniak, K., Geometric Modelling for Numerically Controlled Machining. Oxford University Press, New York 1991.

[10] Peternell, M., Pottmann, H. and Ravani, B., On the computational geometry of ruled surfaces. Comp. Aided Design **31** (1999), 17–32.

[11] Pottmann, H., Peternell, M. and Ravani, B., An introduction to line geometry with applications, Comp. Aided Design **31** (1999), 3–16.

[12] Pottmann, H. and Wallner, J., Computational Line Geometry, Springer-Verlag, to appear 2001.

[13] Ravani, B. and Wang, J.W., Computer aided design of line constructs. J. Mech. Des. **113** (1991) 363–371.

[14] Sauer, R., Differenzengeometrie, Springer, Berlin/Heidelberg, 1970.

[15] Wallner, J. and Pottmann, H., On the geometry of sculptured surface machining, in: Curve and Surface Design: Saint Malo 1999, P.J. Laurent, P. Sablonnière, L.L. Schumaker, eds., Vanderbilt Univ. Press, Nashville, TN, 2000, pp. 417–432.

[16] Wollmann C., Estimation of the principle curvatures of approximated surfaces. Comp. Aided Geom. Design **17** (2000), 621–630.